

Linear-scaling first-principles study of a quasicrystalline molecular material

M. Robinson^{*,a}, P.D. Haynes^b

^a*Theory of Condensed Matter, Cavendish Laboratory, J. J. Thomson Avenue, Cambridge CB3 0HE, UK*

^b*Departments of Physics and Materials, Imperial College London, Exhibition Road, London SW7 2AZ, UK*

Abstract

Quasicrystals exhibit long range order without translational periodicity by siting their constituent atoms on the nodes of a quasiperiodic tiling. Zhou and Harris [Z. Zhou, K.D.M. Harris, *ChemPhysChem* 7 (2006) 1649] have proposed engineering a 2D molecular quasicrystal where each node of a Penrose tiling is occupied by a discrete molecule, the 10,5-coronene. First-principles quantum-mechanical calculations have been performed on the stability and energetics of this molecule using the linear-scaling density-functional theory package ONETEP. The suitability of the 10,5-coronene as a molecular building block is confirmed and different design strategies are compared.

1. Introduction

In 1984 Shechtman *et al.* [1] discovered that rapidly cooled aluminium-manganese alloys had sharp diffraction patterns characteristic of crystals exhibiting fivefold rotational symmetry. However it is well established that a crystalline material with long range periodic order cannot exhibit such a symmetry. This problem was resolved by the fact that some quasiperiodic tilings can exhibit diffraction patterns resembling those found by Shechtman *et al.* By following simple algorithms using a set of predefined tiles these tilings are constructed such that they have long-range order yet do not have translational periodicity.

All examples of quasicrystals found to date are metal alloys. However Zhou and Harris [2] have proposed using discrete molecular building blocks to construct a molecular quasicrystalline material. In such a quasicrystal each node within the tiling is occupied not by an individual atom but an entire molecule. The proposed molecular quasicrystal is based upon the Penrose tiling [3] with a 10,5-coronene (C₃₀H₁₀) occupying each node. This coronene exhibits nearly perfect tenfold symmetry, and is bound to its neighbours via the hydrogen bonds in a carboxylic acid dimer motif. The seven different types of node found within the Penrose tiling are formed by attaching the carboxylic acid substituent at different sites around the coronene (see Fig. 1).

Such a design strategy requires seven different molecules to be present within the quasicrystal. In principle it is possible to use a single coronene molecule with ten substituents at each lattice site rather than the seven molecule strategy. However this would cause clashes between substituents on neighbouring molecules [4] rendering such a

single molecule strategy impractical. It is possible however to avoid such steric clashes using a set containing just three molecules. Such a set not only has the advantage of fewer molecular components but also a significantly higher density more typical of crystalline organic materials.

In this paper we use the Kohn-Sham approach [5] to density-functional theory (DFT) [6] to perform *ab initio* calculations on both single coronenes and coronene dimers to verify their suitability as a basis for building a molecular quasicrystal and to compare design strategies.

2. Methodology

DFT has made a far reaching impact on disciplines ranging from chemistry and materials through to geology and the biological sciences. This has been due to the high accuracy and predictive power of DFT at a computational cost that scales favourably with system size. However conventional DFT codes must maintain the orthogonality of the Kohn-Sham (KS) orbitals. Since these orbitals are delocalised over the entire system, the computational cost in maintaining their orthogonality increases with the cube of the system size. Within the plane-wave pseudopotential (PWP) method the KS orbitals are represented by plane-waves. This has the advantage that all space is represented to the same accuracy without any bias so that no prior knowledge of the electronic structure is required, but comes at the cost of consuming computational resources on vacuum. For this reason maintaining the orthogonality of the KS orbitals within the PWP method for extended systems requiring large simulation cells such as the coronene dimer can become prohibitive even when the number of atoms is relatively small. Over the last decade a number of linear-scaling DFT codes have emerged that overcome this computational bottleneck [7]. In this paper we make use of one such code, ONETEP, to provide *ab initio* results with plane wave accuracy [8].

*Corresponding author. Fax: +44 1223 337356

Email address: mr419@cam.ac.uk (M. Robinson)

ONETEP achieves linear scaling by minimising the total energy calculated from the single-particle density matrix. The density matrix is written in terms of a set of non-orthogonal generalised Wannier functions (NGWFs) [9] that are localised in real space rather than the orthogonal delocalised Kohn-Sham orbitals,

$$\rho(\mathbf{r}, \mathbf{r}') = \sum_{\alpha, \beta} \phi_{\alpha}^{*}(\mathbf{r}) K^{\alpha\beta} \phi_{\beta}(\mathbf{r}'). \quad (1)$$

The energy is then self-consistently minimised with respect to both the density kernel $K^{\alpha\beta}$ and the NGWFs $\{\phi_{\alpha}(\mathbf{r})\}$. To perform the minimisation the NGWFs are written in terms of a basis of periodic cardinal sine (psinc) functions [10] that are themselves constructed from plane waves. NGWFs are localised to spherical regions around the atomic centres and the density kernel truncated to only include NGWFs within a predefined spatial cutoff.

Transformations between real and reciprocal space are performed using the FFT box technique [11] where the FFT is calculated within a localised box around each NGWF rather than within the simulation cell. The volume of the FFT box is only dependent on the cutoff radii of the NGWFs and so the computational cost in performing the FFT does not increase with system size and linear-scaling is maintained. Using this approach ONETEP has been shown to perform linear-scaling calculation on thousands of atoms with plane wave accuracy [12].

The binding energy calculations presented in this paper were made using q_c -tuned norm-conserving pseudopotentials [13] and a revised [14] version of the PBE [15] exchange and correlation functional. NGWFs centred on carbon and oxygen atoms were localised within spheres of radius 7.5 bohr while NGWFs representing hydrogen had cutoff radii of 7.0 bohr. An infinite cutoff was used for the density kernel, effectively preventing any truncation. All calculations were performed in a supercell $80 \times 80 \times 50$ bohr in size. Since the simulation cell is large and therefore the Brillouin zone small, ONETEP is able to achieve accurate results while only sampling at the Γ -point. This has the advantage that the wavefunctions and therefore NGWFs can be chosen to be real. Before recording the total energy the ionic positions of each structure were first allowed to relax using a quasi-Newton method [16]. This was done for both the binding energy and nodal calculations.

The size of the psinc basis set used in ONETEP is determined by the parameter E_{cut} , in a similar manner to plane waves [17]. For the calculations presented in this paper a value of 700 eV for E_{cut} was found to provide suitably converged energies and forces.

3. Results and Discussion

Three aspects of a 10,5-coronene based molecular quasicrystal have been studied. Firstly we study a coronene dimer formed via different substituents to verify that the coronene can form a stable dimer. Secondly we compare

the energetics of the nodes used in the seven and three molecule design strategies. Thirdly we combine our results from the binding and nodal calculations to make predictions of the total energy for two dimensional sheets of quasicrystals based on the different design strategies.

3.1. Coronene Stability

First the stability of a single 10,5-coronene was confirmed by calculating the total energy and atomic forces while distorting the coronene. For all distortions studied the total energy increased and the atomic forces restored the molecule to a planar structure. The slight distortion from perfect D_{10h} symmetry to C_{5h} symmetry that has been seen in previous Hartree-Fock calculations [18] was observed. Although this distortion is likely to be underestimated by DFT it is not significant enough to affect the binding and nodal calculations presented here.

Two coronenes can bind via any number of different substituents bound to the coronene. Here we present binding energies for the two different binding strategies shown in Fig. 1. Firstly the simplest possible chemical link, a carbon chain. Secondly the more complex binding via a carboxylic acid dimer motif where two hydrogen bonds are formed as originally suggested in Zhou and Harris' first paper. The length of the carbon chain was chosen such that it approximately matched the length of the bound carboxylic dimer motif. When calculating the total energy of the unbound coronenes the chain was broken at half its length such that the two unbound molecules were symmetric.

Since the NGWFs are optimised *in situ* during the calculation, ONETEP does not suffer from any basis set superposition error [19]. Hence no counterpoise or any alternative correction is required when comparing two ONETEP calculations on different molecules so long as the underlying psinc basis is the same. As identical simulation cells, NGWF cutoff radii and plane-wave cutoffs have been used for each calculation the total energies from each can be directly compared.

The binding energy of two 10,5-coronenes via a carbon chain was found to be 0.20 eV. This is nearly an order of magnitude larger than kT at room temperature demonstrating the stability of the dimer. Though this result will be subject to a small error due to the failure of DFT to correctly capture the Peierls distortion, it should not be large enough to effect its comparison with the carboxylic acid binding energy. Binding via the carboxylic acid motif was found to be 0.59 eV, three times stronger than via a carbon chain indicating the value in the hydrogen bonds. These results clearly support Zhou and Harris' design strategy of using the carboxylic acid motif as the means of binding two coronenes.

3.2. Nodal Energies

Total energies were calculated for each of the nodes found in the seven molecule design strategy (labelled 1 to 7) and three molecule strategy (labelled A to C), and for an

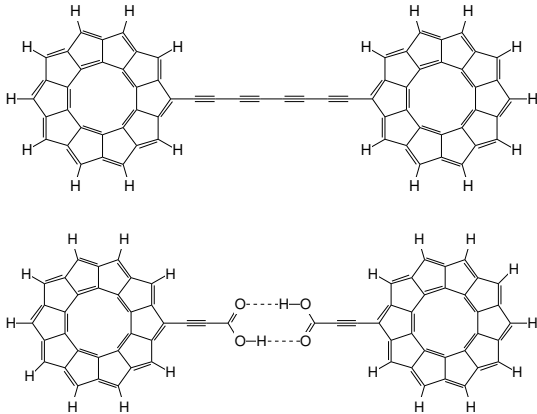


Figure 1: The two modes of dimer binding studied in this work are shown: via a carbon chain (top) and via a carboxylic acid dimer motif (bottom). The seven different node types found in the Penrose tiling are constructed by attaching the substituent at different points around the coronene.

isolated coronene. Each of these nodes are comprised of a number of carboxylic acid substituents bound at different sites around a coronene. The results of these calculations are shown in Table 1. Immediately it is apparent there is a discrepancy between nodes with the same number of substituents bound to the coronene. For example Nodes 1 and 4 both have five substituents yet their energies differ by 0.21 eV. Other examples are Nodes 3 and B, and Nodes 5 and C.

We suggest this is caused by a repulsive interaction between nearest neighbouring substituents on the coronene. To test this hypothesis we propose that the energy of each node can be approximated by,

$$E_{\text{total}} = E_{\text{cor}} + N_{\text{sub}}E_{\text{sub}} + N_{\text{pair}}E_{\text{rep}}. \quad (2)$$

Here N_{sub} is the number of substituents and N_{pair} the number of neighbouring pairs of substituents. The similarity of the total energies for Nodes 6 and 7 suggest that any effect due to next nearest neighbours is minimal and so is ignored here. E_{cor} is the energy of the coronene and E_{rep} the repulsive interaction between neighbouring substituents. E_{sub} is the energy of a substituent, including any change in energy involved in binding to a coronene. N_{sub} and N_{pair} for each node type are shown in Table 1.

Energies for nodes in both the seven and three molecule strategies were fitted to Eq. 2 using a least squares algorithm. The calculated energy of an unbound coronene was used for E_{cor} to minimise parameters in the fitting. E_{sub} was found to be -1337.54(1) eV and E_{rep} to be +0.17(2) eV. The final RMS difference between computed energies and those found using Eq. 2 was 0.12 eV, suggesting that total energies for any given nodal configuration could be predicted to this accuracy.

The positive value of E_{rep} validates the hypothesis that repulsive interactions are present between neighbouring substituents. Consequently those nodes with many neighbouring substituents will be less stable than those with

fewer substituents. This brings into question the stability of the nodes used in the three molecule strategy, all of which have more neighbouring pairs than those nodes they are replacing in the seven molecule strategy.

To further investigate the stability of the nodes, formation energies have been calculated for each. The formation energy is the difference between the total energy and the sum of the energies of all the constituent atoms in their elemental molecular or crystal form. For hydrogen and oxygen atoms the energy of an atom in their dimer was used, for carbon an atom in graphite used. The formation energies of each node are tabulated alongside their total energies in Table 1. It can be seen that all the nodes have negative formation energies, confirming their stability over their elemental environment. However the positive formation energy of the unbound coronene is a concern, raising the question of whether the 10,5-coronene would be stable in practice. A formation energy of +10.06 eV is likely due to the molecule containing so many pentagonal rings. To the authors' knowledge there has never been any reported synthesis of this molecule.

3.3. Bulk Energies

Using the results for the binding energy of a coronene dimer, the total energies of each node, and the relative frequencies of occurrence for each node, it is possible to predict total energies for a 2 dimensional sheet of the molecular quasicrystal,

$$E_{\text{bulk}} = \sum_{\text{nodes}} f_n(E_n + \frac{1}{2}N_{\text{bond},n}E_{\text{bind}}). \quad (3)$$

The total energy per node is calculated as a sum over the seven node types in a Penrose tiling. Each node n of energy E_n occurs with frequency f_n and forms $N_{\text{bond},n}$ bonds with energy E_{bind} . A factor of a half is included to prevent double counting bonds. For the three molecule strategy Nodes A and B will appear more than once in the sum since they represent more than one node type in the Penrose tiling. Using the total energies and frequencies tabulated in Table 1 and the binding energy calculated in Section 3.1 the average energy per node was found to be -10181.45 eV for the seven molecule strategy and -15140.28 eV for the three molecule strategy. The dramatic difference in energy between the two strategies is attributed to the nodes within the three molecule strategy simply containing more atoms and so each molecule contributing a lower energy.

To make a comparison of the two design strategies that is not biased by the difference in molecular sizes of the nodes we now consider just the interaction energies. We have observed two dominant contributions to the energy from molecular interactions within the 2D quasicrystal. Each bond between two coronenes lowers the energy, while the repulsion between neighbouring substituents on each node raises the energy. Using the values for these two contributions calculated in Section 3.1 and Section 3.2 the

		N_{sub}	N_{pair}	Total Energy / eV	Formation Energy / eV	Relative Frequency
10,5-Coronene		0	0	-4830.16	+10.06	-
Node 1		5	0	-11517.78	-7.25	τ
Node 2		6	2	-12854.90	-10.32	1
Node 3		7	4	-14192.25	-13.60	τ
Node 4		5	2	-11517.57	-7.04	τ^4
Node 5		4	0	-10180.30	-3.84	τ^2
Node 6		3	0	-8842.91	-0.50	τ^5
Node 7		3	0	-8842.93	-0.52	τ^3
Node A		10	10	-18203.87	-23.04	$1 + 2\tau + \tau^4$
Node B		7	6	-14192.02	-13.37	$\tau^2 + \tau^5$
Node C		4	2	-10180.19	-3.72	τ^3

Table 1: Schematic diagrams for each nodal configuration studied are tabulated alongside their total energies and formation energies. The blue circles represent the coronene, while each red line indicates a carboxylic acid substituent. Dotted lines indicate where a substituent has been added purely to increase the density, rather than to form a bond. Nodes used in the seven molecule design strategy are labelled numerically, while those used in the three molecule strategy are labelled alphabetically. In the three molecule strategy molecules represent more than one node type: Node A takes the place of Nodes 1 to 4, Node B takes the place of Nodes 5 and 6, and Node C takes the place of Node 7. The number of substituents N_{sub} , the number of neighbouring pairs of substituents N_{pair} , and the relative frequency of occurrence for each node type is also shown. Energies are given in eV and τ is the golden ratio, $(1 + \sqrt{5})/2$.

average interaction energy per node due to these interactions can be computed,

$$E_{\text{inter}} = \sum_{\text{nodes}} f_n(N_{\text{pair},n}E_{\text{rep}} + \frac{1}{2}N_{\text{bond},n}E_{\text{bind}}). \quad (4)$$

The interaction energy was found to be -1.06 eV for the seven molecule strategy and -0.03 eV for the three molecule strategy. The seven molecule strategy clearly wins over the three molecule strategy under this analysis as its nodes have far fewer neighbouring substituents. For the three molecule strategy the energy loss due to binding and energy gain due to repulsive interactions are roughly comparable.

The molecules used in the three molecule strategy were designed to increase the density and so both Nodes B and C contain substituents that are never involved in bonding yet add to the repulsion term. A compromise between

the two strategies would be to remove these substituents decreasing the density slightly but increasing the stability. Such a reduced three molecule strategy would use Node 7 in the place of Node C, and Node B would only contain five substituents with two neighbouring pairs. Using Eq. 2 the total energy of the reduced Node B is predicted to be -11517.54 eV. This gives an average total energy per node of -13682.46 eV, and an average interaction energy per node of -0.35 eV. The chemist synthesising a coronene based quasicrystal will have to weigh up the benefits of fewer molecular components and the higher density obtained with the three molecule strategies with the increased interaction energy and therefore lower stability.

4. Conclusions

Since the discovery of quasicrystals by Shechtman *et al.* a number of materials exhibiting diffraction patterns with symmetries previously regarded incompatible with long range order have been discovered and synthesised. However to date none of these materials has been a molecular material. We have verified the design strategy of the 2D molecular quasicrystal proposed by Zhou and Harris finding that all the molecules involved are stable, though the 10,5-coronene that these molecules are based on has been found to have a positive formation energy. The two hydrogen bonds formed in the coronene dimer provide a binding energy an order of magnitude greater than kT at room temperature. The average total energies per node for the two design strategies proposed have been computed. A repulsive interaction between neighbouring carboxylic acid motifs bound to a coronene was found compromising the stability of nodes with many neighbouring substituents. Since the nodes within the three molecules strategy have far more neighbouring substituents this suggests that when synthesising such a material a compromise will have to be made. The advantages of a smaller set of molecules and denser material obtained using a three molecule strategy will have to be weighed up against the lower stability compared to the seven molecule strategy.

These results introduce ONETEP to a new class of system, 2D materials, and demonstrate its suitability for investigating materials that require very large simulation cells. Since quasicrystals are not periodic it will only ever be possible to model a fragment of such a material and never to model it in bulk using periodic boundary conditions. However since ONETEP scales linearly with system size it would be well within the computational resources currently available to the authors to model far larger fragments than the dimer studied in this paper. Indeed it should be possible using modern supercomputing facilities to model fragments sufficiently large that bulk properties could be observed.

Acknowledgements

We are grateful to Dr Zhongfu Zhou for introducing us to this topic. M.R. would like to thank the EPSRC for a Ph.D. studentship and P.D.H. the Royal Society for a University Research Fellowship.

References

- [1] D. Shechtman, I. Blech, D. Gratias, J.W. Cahn, Phys. Rev. Lett. 53 (1984) 1951.
- [2] Z. Zhou, K.D.M. Harris, ChemPhysChem 7 (2006) 1649.
- [3] R. Penrose, Bull. Inst. Math. Appl. 10 (1974) 266.
- [4] Z. Zhou, K.D.M. Harris, J. Phys. Chem. C 112 (2008) 16186.
- [5] W. Kohn, L.J. Sham, Phys. Rev. 140 (1965) 1133.
- [6] P. Hohenberg, W. Kohn, Phys. Rev. 136 (1964) 864.
- [7] S. Goedecker, Rev. Mod. Phys. 71 (1999) 1085.
- [8] C.-K. Skylaris, P.D. Haynes, A.A. Mostofi, M.C. Payne, J. Chem. Phys. 122 (2005) 084119.
- [9] C.-K. Skylaris, A.A. Mostofi, P.D. Haynes, O. Diéguez, M.C. Payne, Phys. Rev. B 66 (2002) 035119.
- [10] A.A. Mostofi, P.D. Haynes, C.-K. Skylaris, M.C. Payne, J. Chem. Phys. 119 (2003) 8842.
- [11] A.A. Mostofi, C.-K. Skylaris, P.D. Haynes, M.C. Payne, Comput. Phys. Commun. 147 (2002) 788.
- [12] C.-K. Skylaris, P.D. Haynes, J. Chem. Phys. 127 (2007) 164712.
- [13] V. Milman, M.-H. Lee, J. Chem. Phys. 100 (1996) 6093.
- [14] B. Hammer, L.B. Hansen, J.K. Norskov, Phys. Rev. B 59 (1999) 7413.
- [15] J.P. Perdew, K. Burke, M. Ernzerhof, Phys. Rev. Lett. 77 (1996) 3865.
- [16] B.G. Pfrommer, M. Cote, S.G. Louie, M.L. Cohen, J. Comput. Phys. 131 (1997) 233.
- [17] C.-K. Skylaris, P.D. Haynes, A.A. Mostofi, M.C. Payne, J. Phys.: Condens. Matter 17 (2005) 5757.
- [18] G. Monaco, R.G. Viglione, R. Zanasi, P.W. Fowler, J. Phys. Chem. A 110 (2006) 7447.
- [19] P.D. Haynes, C.-K. Skylaris, A.A. Mostofi, M.C. Payne, Chem. Phys. Lett. 422 (2006) 345.